Supporting information for:

Chemical Phosphoproteomics Sheds New Light on the Targets and Modes of Action of AKT Inhibitors

Svenja Wiechmann[1,2,3], Benjamin Ruprecht[1,§], Theresa Siekmann[1], Runsheng Zheng[1,%], Martin Frejno[1,$], Elena Kunold[4,&], Thomas Bajaj[5], Daniel P. Zolg[1,$], Stephan A. Sieber[4], Nils C. Gassen[5], Bernhard Kuster[1,2,3,6,*]

[1] Chair of Proteomics and Bioanalytics, Technical University of Munich, 85354 Freising, Germany
[2] German Cancer Consortium (DKTK), 80336 Munich, Germany
[3] German Cancer Center (DKFZ), 69120 Heidelberg, Germany
[4] Organic Chemistry II, Technical University of Munich, 85748 Garching, Germany
[5] Department of Psychiatry, Bonn Clinical Center, 53127 Bonn, Germany
[6] Bavarian Center for Biomolecular Mass Spectrometry, 85354 Freising, Germany

[§] Present address: Chemical Biology, Merck Research Laboratories, Boston, MA 02115, USA
[%] Present address: Thermo Fisher Scientific, 82110 Germering, Germany
[$] Present address: MSAID GmbH, 85748 Garching, Germany
[&] Present address: SciLifeLab, 17 165 Solna, Sweden

[*] Corresponding author: Bernhard Kuster, kuster@tum.de

Contents

Online Methods

Small molecule inhibitors. AKT modulators VIII (#14870) and SC79 (#14972) were from Cayman Chemical. PHT-427 (#P3076) was obtained from LKT Laboratories. AZD5363 (#S8019), GSK2110183 (#S7521) GSK690693 (#S1113), Ipatasertib (#2808), MK-2206 (#S1078), Perifosine (#S1037) and Miransertib (#S8339) were from Selleckchem. Uprosertib (#A-1504) was purchased from Active Biochem. Lapatinib (#SML2259) was purchased from Sigma-Aldrich.

Cell culture and kinase inhibitor treatment. BT-474 cells were cultured in DMEM/Hams F-12 (1:1) with 10 % FBS and 1 % antibiotic and antimycotic solution (Biochrom) at 37 °C and 5 % CO_2 according to standard cell culture methods. Cell line authentication was accomplished by short tandem repeat (STR) profiling (Multiplexion) [1]. For kinase inhibitor treatments, BT-474 cells were grown until a 70 % confluency was reached. 1 h prior to the treatment, the medium was exchanged. Subsequently, fresh medium supplemented with kinase inhibitor at the indicated concentration was added to the cells which were further incubated at 37 °C for the indicated times.

Cell viability assay with alamarBlue reagent. 2 x 10^4 cells of BT-474 cells were seeded into a 96-well microtiter plate in quadruplicate for each inhibitor and incubated at 37 °C and 5 % CO_2. After 24 h, dilutions of the kinase inhibitors (10 µM, 3 µM, 1 µM, 300 nM, 100 nM, 30 nM, 10 nM, 3 nM, 1 nM) in medium were added to the cells. After a 72 h treatment, alamarBlue reagent (Thermo Fisher Scientific) was added 1:10 to each well. The fluorescence was quantified at $\lambda_{excitation}$ = 544 nm and $\lambda_{emission}$ = 584 nm on the microplate reader FluoStar Omega (BMG Labtech).

Protein concentration assay. The protein concentration in cell lysate was determined using the Coomassie Plus Bradford (Thermo Fisher Scientific) assay according to the protocol of the manufacturer.

Sample preparation for kinase selectivity profiling. For the analysis of kinase inhibitor targets in BT-474 cells, kinobead γ-pulldowns were performed as previously described [2]. Briefly, cells were lysed in 0.8 % NP40, 50 mM Tris-HCl pH 7.5, 5 % glycerol, 1.5 mM $MgCl_2$, 150 mM NaCl, 1 mM Na_3VO_4, 25 mM NaF, 1 mM DTT, protease inhibitors (SigmaFast, Sigma) and phosphatase inhibitors. Designated AKT inhibitors were spiked into 1 mL of lysate, which was adjusted to 5 mg/mL protein, with increasing concentrations (DMSO control, 3 nM, 10 nM, 30 nM, 100nM, 300nM, 1 µM, 3 µM, 10 µM and 30 µM) and incubated for 45 min at 4°C. Afterwards, incubation with 35 µL settled kinobeads took place for 30 min at 4 °C. In order to enable the determination of a correction factor for each protein and to calculate apparent dissociation constants, a second kinobead pulldown (with fresh beads) was performed on the unbound fraction of the DMSO control. Proteins bound to kinobeads were eluted with LDS sample buffer (NuPAGE, Thermo Fisher Scientific) containing 50 mM DTT and alkylated with 55 mM CAA. Kinobead pulldown eluates were purified by short SDS-PAGE (ca. 1 cm; Thermo Fisher Scientific) and were subsequently subjected to in-gel tryptic digestion according to standard procedures. After drying in a centrifugal evaporator, the samples were stored at -20 °C until LC-MS/MS analysis.

Sample preparation for TMT-DDA phosphoproteomic analysis and PRM assay. After treatment with designated AKT inhibitors, BT-474 cells were washed twice with PBS and lysed in 40 mM Tris-HCl pH 7.6, 8 M urea, EDTA-free protease inhibitor (Roche) and phosphatase inhibitors (Roche). Lysate was centrifuged for 1 h at 21,000 x g and the supernatant was subjected to further processing. 2 mg protein of BT-474 lysate was reduced

with 10 mM DTT for 40 min at 56 °C and alkylated with 25 mM CAA at room temperature in the dark for 20 min. After dilution of the urea concentration from 6 M to 1.5 M with 40 mM Tris-HCl pH 7.6, the proteins were digested in a 1:100 trypsin/substrate weight ratio for 4 h at 37 °C and 700 rpm. The second digestion step was performed overnight again in a 1:100 trypsin/substrate weight ratio in presence of 1 mM $CaCl_2$. Desalting of tryptic peptides was performed on Sep-Pak C18 50 mg columns (Waters) as described elsewhere in 0.07 % TFA in 50 % ACN. P-peptides were enriched using Fe-IMAC as previously described [3]. P-peptides were further desalted by using 0.07 % TFA in 50 % ACN in the micro-column format (three discs, Ø 1.5 mm, C18 material, 3M Empore per micro-column were used) as described [4]. After adding an equivalent of 500 fmol Pierce Retention Time Calibration Mixture (Thermo Fisher Scientific) for each MS injection to each PRM sample, sample preparation for label-free PRM assays was completed at this point. P-peptides for TMT-DDA analysis were labeled using TMT 6-plex at a final concentration of 6.67 mM according to instructions provided by the manufacturer. One TMT channel was used for each treatment condition (126 = control, 127 = AZD5363, 128 = GSK2110183, 129 = GSK690693, 130 = ipatasertib, 131 = MK-2206). Subsequently, peptides were separated into six fractions using basic reversed-phase fractionation in micro-column format (five discs, Ø 1.5 mm, C18 material, 3M Empore per micro-column were used) in 25 mM NH_4COOH (pH 10). Peptides were fractionated with increasing ACN concentrations (5 %, 7.5 %, 10 %, 12.5 %, 15 %, 17.5 % and 50 % ACN). The desalted flow-through was combined with the 17.5 % fraction and the 50 % fraction with the 5 % fraction to give a total of six fractions. After drying in a centrifugal evaporator, the samples were stored at -20 °C until LC-MS^3 analysis.

Peptide synthesis. Peptides were designed as 15-mers (11-mer for Crosstide) with Serine or Alanine in the central position for wildtype or mutant, respectively, with a free N–terminal amino group and a C–terminal amide group. The synthesis was performed by an automated

peptide synthesizer (Intavis Bioanalytical Instruments AG) in 2 µmol-scale by applying Fmoc chemistry. Purity was analyzed by MALDI–TOF–MS on an UltrafleXtreme (Bruker).

In vitro AKT2 assay. Peptide pools were added to 20 mM HEPES-KOH pH 7.4, 5 mM $MgCl_2$, 1 mM DTT and 2 mM ATP to reach an end concentration of 6 µM. The reaction was started by supplementing 12.5 ng/µl recombinant active AKT2 (Jena Bioscience, #PR-333,) and was incubated at 30 °C for different times (0, 5, 10, 30, 60, 120, 180 min). The reaction was quenched by adding an equal volume of 1 % FA in ACN. After drying in a centrifugal evaporator, the samples were stored at -20 °C until LC-MS/MS analysis.

LC-MS^n measurements

Kinome. Nano-flow LC-MS/MS measurement of peptides in Kinobead eluates was performed using a nanoLC-Ultra 1D+ (Eksigent) coupled to a LTQ Orbitrap Elite mass spectrometer (Thermo Fisher Scientific). Peptides were desalted on a trap column (100 µm × 2 cm, packed in-house with Reprosil-Pur C18-AQ 5 µm resin; Dr. Maisch) in 0.1 % FA at 5 µl/min and separated on an analytical column (75 µm × 40 cm, packed in-house with Reprosil-Pur C18-AQ, 3 µm resin; Dr. Maisch) using a 100 min linear gradient from 4-32 % solvent B (0.1 % formic acid, 5 % DMSO in ACN) in solvent A1 (0.1 % formic acid, 5 % DMSO in water) at a flow rate of 300 nL/min. The mass spectrometer was operated in data dependent acquisition and positive ionization mode. MS1 spectra were acquired over a range of 360-1300 m/z at a resolution of 30,000 (at m/z 400) in the orbitrap and an automatic gain control (AGC) target value of $1x10^5$. Up to 15 peptide precursors were selected for fragmentation by higher energy collision-induced dissociation (HCD; isolation width of 2 Th, maximum injection time of 100 ms, AGC value of $2\ x10^5$) using 30 % normalized collision energy (NCE) and analyzed in the orbitrap (7,500 resolution).

TMT6 phosphoproteome. Nano-flow LC-MS^3 measurement of TMT-labeled p-peptides was performed using a Dionex Ultimate3000 nano HPLC (Thermo Fisher Scientific) coupled to an orbitrap Fusion mass spectrometer (Thermo Fisher Scientific). Peptides were desalted on a trap column (Acclaim C18 PepMap100, 75 µm i.d. ×2 cm; Thermo Fisher Scientific) in 0.1 % FA and separated on an analytical column (Acclaim C18 PepMap RSLC, 75 µM i.d. ×15 cm; Thermo Fisher Scientific) using a 120 min gradient from 3-25 % B (0.1 % FA, 5 % DMSO in 100 % ACN) in solution A (0.1 % FA, 5 % DMSO in water). The Fusion was operated in data dependent acquisition and positive ionization mode. Full scan MS1 spectra were acquired over a range of 300-1700 m/z at a resolution of 60,000 (AGC target value 4x10^5, maximal injection time 50 ms). Fragmentation was performed using CID at 40 % NCE and MS2 spectra acquisition (AGC target value 4 x10^4, maximal injection time 60 ms) took place in the ion trap. For TMT quantification an additional MS3 spectrum was acquired in the orbitrap over an m/z range of 100-500 at 60,000 resolution for each peptide precursor. For this, fragment ions were selected by multi-notch isolation, allowing a maximum of 10 notches and an ion trap isolation width of 2 Da, and subsequently fragmented by HCD at 55 % NCE (AGC target value 1 x10^5, maximal injection time 120 ms).

In vitro kinase assay. Nano-flow LC-MS/MS measurement of peptides deriving from the in vitro kinase assay was performed using a Dionex Ultimate3000 nano HPLC (Thermo Fisher Scientific) coupled to an orbitrap Fusion Lumos mass spectrometer (Thermo Fisher Scientific). Peptides were desalted on a trap column (100 µm × 2 cm, packed in-house with Reprosil-Pur C18-AQ 5 µm resin; Dr. Maisch) in 0.1 % FA and separated on an analytical column (75 µm × 40 cm, packed in-house with Reprosil-Pur C18-AQ, 3 µm resin; Dr. Maisch) using a 51 min two-step gradient from 4-15-27 % B (0.1 % FA, 5 % DMSO in 100 % ACN) in solution A (0.1 % FA, 5 % DMSO in water). The Fusion Lumos was operated in data dependent acquisition and positive ionization mode. Full scan MS1 spectra were acquired over a range of 360-1300 m/z at a resolution of 60,000 (AGC target value 5 x10^4, maximal

injection time 50 ms). Fragmentation was performed using HCD at 30 % NCE (AGC target value 5 $x10^4$, maximal injection time 120 ms) in the orbitrap at 30,000 resolution.

PRM assay. Nano-flow LC-MS/MS measurement of peptides for generating a spectral library and the PRM assay was performed using a Dionex Ultimate3000 nano HPLC (Thermo Fisher Scientific) coupled to an orbitrap Fusion Lumos mass spectrometer (Thermo Fisher Scientific). Peptides were desalted and separated as described for in vitro kinase assay samples, except for a longer gradient of 110 min for the spectral library generation. The Fusion Lumos was operated in data dependent acquisition and positive ionization mode. For generating the spectral library, full scan MS1 spectra were acquired over a range of 360-1300 m/z at a resolution of 60,000 (AGC target value 4 $x10^5$, maximal injection time 50 ms). Targeted MS2 scans were acquired over a range of 120-2000 m/z and fragmentation was performed using HCD at 30 % NCE (AGC target value 1 $x10^5$, maximal injection time 50 ms) in the orbitrap at 15,000 resolution by taking into account the mass list of p-peptides. For the PRM assay, full scan MS1 spectra were acquired over a range of 360-1300 m/z at a resolution of 15,000 (AGC target value 4 $x10^5$, maximal injection time 50 ms). Targeted MS2 scans were acquired over a range of 120-2000 m/z and fragmentation was performed using HCD at 30 % NCE (AGC target value 2e5, maximal injection time 100 ms) in the Orbitrap at 15,000 resolution by taking into account the final mass list of p-peptides (Table S5).

Database searching and data analysis.

Protein and peptide identification and quantification was performed using MaxQuant [5] (version 1.5.6.5). If not stated otherwise, the MS data was searched against all human canonical and isoform protein sequences as annotated in the Swissprot reference database (42,095 entries, downloaded 14.11.2016) using the embedded search engine Andromeda [6].

Kinome. Carbamidomethylated cysteine was a fixed modification; and phosphorylation of serine, threonine, and tyrosine, oxidation of methionine, and N-terminal protein acetylation

were variable modifications. Trypsin/P was specified as the proteolytic enzyme and up to two missed cleavage sites were allowed. Precursor and fragment ion tolerances were 4.5 ppm and 20 ppm, respectively. Label-free quantification [7] and match-between-runs were enabled within MaxQuant. Protein intensities were normalized to the respective DMSO control. IC50 and EC50 values were calculated by a four-parameter log-logistic regression using an internal pipeline that utilizes the 'drc' [8] package in R. A K_d^{app} was computed by multiplying the estimated EC50 with a protein-dependent correction factor that was limited to a maximum value of 1. The correction factor for a protein is defined as the ratio of the amount of protein captured from two consecutive pulldowns of the same DMSO control lysate [2] and was set to the average of correction factors across all experiments using the same lysate and beads.

TMT6 phosphoproteome. Carbamidomethylated cysteine was a fixed modification; and phosphorylation of serine, threonine, and tyrosine, oxidation of methionine, and N-terminal protein acetylation were variable modifications. Trypsin/P was specified as the proteolytic enzyme and up to two missed cleavage sites were allowed. Precursor and fragment ion tolerances were 5 ppm and 0.5 Da, respectively. MS3-based TMT quantification was enabled, taking TMT correction factors as supplied by the manufacturer into account. Further phosphorylation events on the respective underlying tryptic peptide were considered for the p-site identifications (as indicated by a multiplicity greater than 1 in the Phospho (STY)Sites.txt). Within one replicate, the sum of p-site intensities per TMT channel were normalized to the average sum of intensities of all TMT channels. Subsequently, the average intensities for each phosphorylation site per replicate was normalized to the average intensity of the same phosphorylation site across all replicates. Data was further analyzed by Perseus (version 1.5.5.3) [9]. Only p-sites which were identified and quantified in at least three out of four replicates were considered for further analysis. Log_2 FC for each inhibitor against the vehicle control were calculated per phosphorylation site and tested for significance using a t-test (permutation-based FDR; randomizations = 250, FDR = 5 %, s0 = 0.1). Protein-protein

interactions were analyzed using the String database [10] (version 11.0) (combined score > 0.4) and visualized in Cytoscape (version 3.4.0). Frequency sequence logos were generated using WebLogo [11] (available from http://weblogo.berkeley.edu/).

In vitro kinase assay. Peptide identification and quantification was performed by searching the MS data against a database containing only sequences of the screened peptides. Phosphorylation of serine and threonine, oxidation of methionine, and N-terminal protein acetylation were set as variable modifications. Precursor and fragment ion tolerances were 4.5 ppm and 20 ppm, respectively. Peptide-spectrum-match intensities for each peptide were summed, with the prerequisite that the peptide was identified in at least two out of three replicates. Only those PSMs of p-peptides with a higher localization probability of the intended p-site than another p-site were considered for summing up peptide intensity. The intensity of each peptide across experiments was further normalized to the total peptide intensity in each experiment.

PRM assay. In order to obtain the spectral library, respective raw files were searched in MaxQuant with carbamidomethylated cysteine as a fixed modification; and phosphorylation of serine, threonine, and tyrosine, oxidation of methionine, and N-terminal protein acetylation as variable modifications. Trypsin/P was specified as the proteolytic enzyme and up to two missed cleavage sites were allowed. Precursor and fragment ion tolerances were 10 ppm and 4.5 ppm, respectively. The PRM raw data files were imported into the Skyline software package (version 4.1.0.11714) [12]. Confident p-peptide identification was carried out based on iRT information using spiked-in retention time peptides, matching relative transition intensities between the PRM peak and the library MS2 spectrum (if available) and requiring site determining ions for each phosphorylation site. For accurate p-peptide quantification, low-quality or interfered transitions were discarded manually. Peaks were integrated using the automatic peak finding function followed by the manual curation of all peak boundaries. By calculating the sums of all transition areas associated with the p-peptide, quantification of

each p-peptide was accomplished. Peak areas were normalized based on the total MS1 intensity across the experiments. Log_2 FC for each inhibitor against the vehicle control were calculated per p-peptide. The median log2 FC of the 13 quantified p-peptides for each inhibitor were computed to obtain a simple AKT perturbation score.

Western blots. Protein lysates were generated by either harvesting cells in urea (40 mM Tris-HCl pH 7.6, 8 M urea) or RIPA lysis buffer (150 mM NaCl, 1 % IGEPAL CA-630, 0.5 % Sodium deoxycholate, 0.1 % SDS in 50 mM Tris (pH8.0)), supplemented with protease inhibitor (Merck Millipore or Sigma) and phosphatase inhibitor cocktail (Roche). Proteins were separated by SDS-PAGE and electro-transferred onto PVDF membranes. Blots were stored in Tris-buffered saline, supplemented with 0.05 % Tween (TBS-T) and 5 % non-fat milk or 2 % BSA for 1 h at room temperature and then incubated with primary antibody (diluted in TBS/0.05 % Tween, 5 % non-fat milk or BSA) overnight at 4 ºC.
The following primary antibodies were used: β-Actin (1:1000, Santa Cruz Biotechnology, #sc-47778), Phospho-AKT (Thr308) (1:1000, Cell Signaling Technology, #13038), Phospho-AKT (Ser473) (1:1000, Cell Signaling Technology, #4060), AKT (1:1000, Cell Signaling Technology, #9272), Phospho-ATG14 (Ser29) (1:1000, Cell Signaling Technology, #13155), ATG14 (1:1000, Cell Signaling Technology, #5504), Phospho-BECN1 (Ser15) (1:500, Cell Signaling Technology, #84966), Phospho-BECN1 (Ser295) (1:500, Phospho Solutions, #p117-295), BECN1 (1:1000, Cell Signaling Technology, #3738), GAPDH (1:1000, Cell Signaling Technology, #5174), LC3-B (1:1000, Cell Signaling Technology, #3868), SQSTM1/p62 (1:1000, Cell Signaling Technology, #5114),
Phospho-ULK1 (Ser555) (1:1000, Cell Signaling Technology, #5869), Phospho-ULK1 (Ser757) (1:1000, Cell Signaling Technology, #14202), ULK1 (1:1000, Cell Signaling Technology, #8054). Subsequently, blots were washed in TBS-T and probed with the corresponding fluorophore-conjugated or horseradish peroxidase-conjugated secondary

antibody for 3 h at room temperature. The immuno-reactive signals were detected either directly by excitation of the respective fluorophore or by using ECL detection reagent (Millipore). Acquisition and quantification of the band intensities were carried out with the Odyssey (Licor) or ChemiDoc MP (BioRad) imaging systems and respective softwares. Intensities of proteins were normalized to input ACTB and phosphorylated proteins were normalized to the intensity of the respective total protein. Co-immunoprecipitated protein intensity was normalized to the corresponding immunoprecipitated protein intensity.

LC3 autophagic flux assay. To determine the effect of MK-2206 on autophagic flux, BafA1 (Alfa Aesar, #J61835), a specific inhibitor of vacuolar H+-ATPases interfering with lysosomal pH and thereby degradation of autophagosome cargo, was applied on BT-474 cells, 2 h prior lysis. The adequate concentration of BafA1 was previously determined by titration of BafA1 onto BT-474 cells. For quantification of lipidated LC3B, the intensity of LC3B-II was always related to the signal intensity of the corresponding LC3B-I.

Co-Immunoprecipitation of BECN1. BT-474 cells were lysed using CoIP-buffer containing 20 mM Tris-HCl pH 8.0, 100 mM NaCl, 1 mM EDTA, 0.5% IGEPAL CA-630 complemented with protease inhibitor cocktail (Sigma) and phosphatase inhibitor (Roche). The lysate was incubated on an overhead shaker for 20 min at 4 °C. 1.2 mg of protein extract was supplemented with 2.5 µg BECN1 antibody overnight at 4 °C, while rotating. 20 µl of BSA-cleared Protein G Dynabeads (Invitrogen, 100-03D) were added to the lysate–antibody mix followed by 3 h incubation at 4 °C, while rotating. The beads were washed 3 times with cold PBS. Protein-antibody complexes were eluted by boiling for 5 min at 95 °C in 60 µL Laemmli loading buffer. 15 µg of the cell lysates or 5 µl of the immunoprecipitates were separated by SDS-PAGE and visualized by Western Blotting.

Analysis of ATG14 oligomerization. The PBS-washed cell pellet was incubated with 75 µM disuccinimidyl subernate (DSS, Thermo Fisher Scientific, 21655) or corresponding vehicle (DMSO) in PBS. Crosslinking was performed for 30 min at room temperature and subsequent incubation for 2 h at 4 °C, while rotating. After washing with cold PBS, crosslinking was quenched in cold TBS (pH 7.0) for 20 min at 4 °C. For detection of ATG14 oligomerization, lysates were analyzed by capillary electrophoresis on Wes™ (ProteinSimple) using the 60-440 kDa cartridges.

References

1. Castro, F., Dirks, W. G., Fahnrich, S., Hotz-Wagenblatt, A., Pawlita, M., and Schmitt, M. (2013) High-throughput SNP-based authentication of human cell lines, *Int J Cancer 132*, 308-314.
2. Medard, G., Pachl, F., Ruprecht, B., Klaeger, S., Heinzlmeir, S., Helm, D., Qiao, H., Ku, X., Wilhelm, M., Kuehne, T., Wu, Z., Dittmann, A., Hopf, C., Kramer, K., and Kuster, B. (2015) Optimized chemical proteomics assay for kinase inhibitor profiling, *J Proteome Res 14*, 1574-1586.
3. Ruprecht, B., Koch, H., Medard, G., Mundt, M., Kuster, B., and Lemeer, S. (2015) Comprehensive and reproducible phosphopeptide enrichment using iron immobilized metal ion affinity chromatography (Fe-IMAC) columns, *Mol Cell Proteomics 14*, 205-215.
4. Rappsilber, J., Mann, M., and Ishihama, Y. (2007) Protocol for micro-purification, enrichment, pre-fractionation and storage of peptides for proteomics using StageTips, *Nat Protoc 2*, 1896-1906.
5. Cox, J., and Mann, M. (2008) MaxQuant enables high peptide identification rates, individualized p.p.b.-range mass accuracies and proteome-wide protein quantification, *Nature biotechnology 26*, 1367.
6. Cox, J., Neuhauser, N., Michalski, A., Scheltema, R. A., Olsen, J. V., and Mann, M. (2011) Andromeda: a peptide search engine integrated into the MaxQuant environment, *J Proteome Res 10*, 1794-1805.
7. Cox, J., Hein, M. Y., Luber, C. A., Paron, I., Nagaraj, N., and Mann, M. (2014) Accurate proteome-wide label-free quantification by delayed normalization and maximal peptide ratio extraction, termed MaxLFQ, *Mol Cell Proteomics 13*, 2513-2526.
8. Ritz, C., Baty, F., Streibig, J. C., and Gerhard, D. (2015) Dose-Response Analysis Using R, *PLoS One 10*, e0146021.
9. Tyanova, S., Temu, T., Sinitcyn, P., Carlson, A., Hein, M. Y., Geiger, T., Mann, M., and Cox, J. (2016) The Perseus computational platform for comprehensive analysis of (prote)omics data, *Nat Meth 13*, 731-740.
10. Szklarczyk, D., Morris, J. H., Cook, H., Kuhn, M., Wyder, S., Simonovic, M., Santos, A., Doncheva, N. T., Roth, A., Bork, P., Jensen, L. J., and von Mering, C. (2017) The STRING database in 2017: quality-controlled protein-protein association networks, made broadly accessible, *Nucleic Acids Res 45*, D362-d368.
11. Crooks, G. E., Hon, G., Chandonia, J. M., and Brenner, S. E. (2004) WebLogo: a sequence logo generator, *Genome research 14*, 1188-1190.
12. MacLean, B., Tomazela, D. M., Shulman, N., Chambers, M., Finney, G. L., Frewen, B., Kern, R., Tabb, D. L., Liebler, D. C., and MacCoss, M. J. (2010) Skyline: an open source document editor for creating and analyzing targeted proteomics experiments, *Bioinformatics (Oxford, England) 26*, 966-968.

Supporting Figures

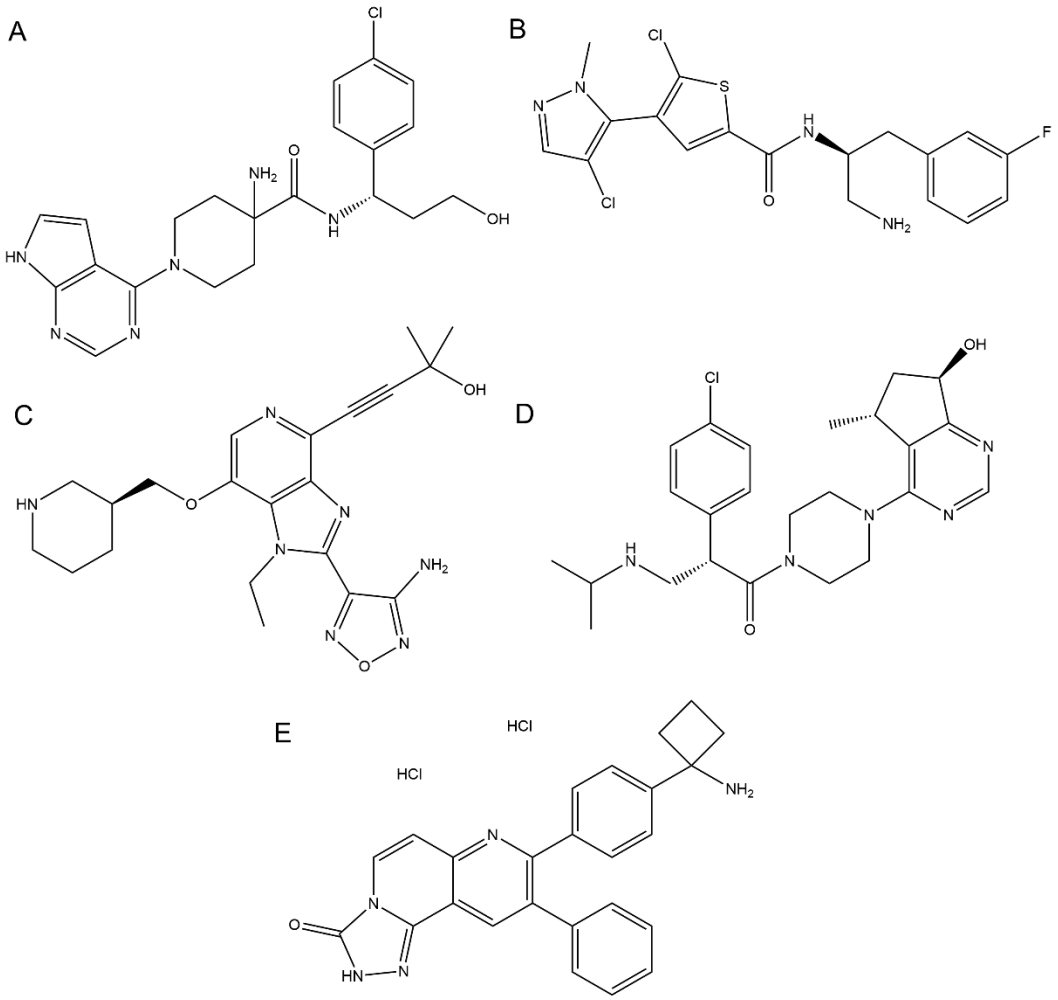

Figure S1: Chemical structures of the analyzed AKT inhibitors.

The chemical structures of **(A)** AZD5363, **(B)** GSK2110183, **(C)** GSK690693, **(D)** Ipatasertib and **(E)** MK-2206 are displayed.

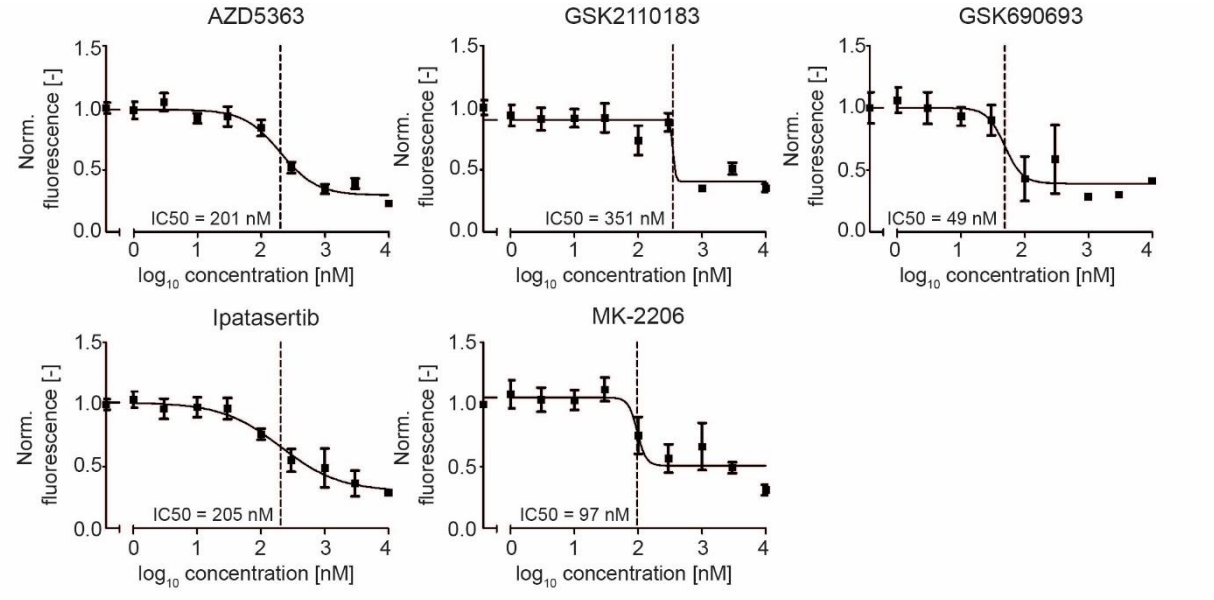

Figure S2: Cell viability assays of BT-474 cells in response to AKT inhibitors.

The drug concentration necessary to reduce cell viability by 50% (IC50) is highlighted by a dashed line. Data represent N = 3 independent biological replicates.

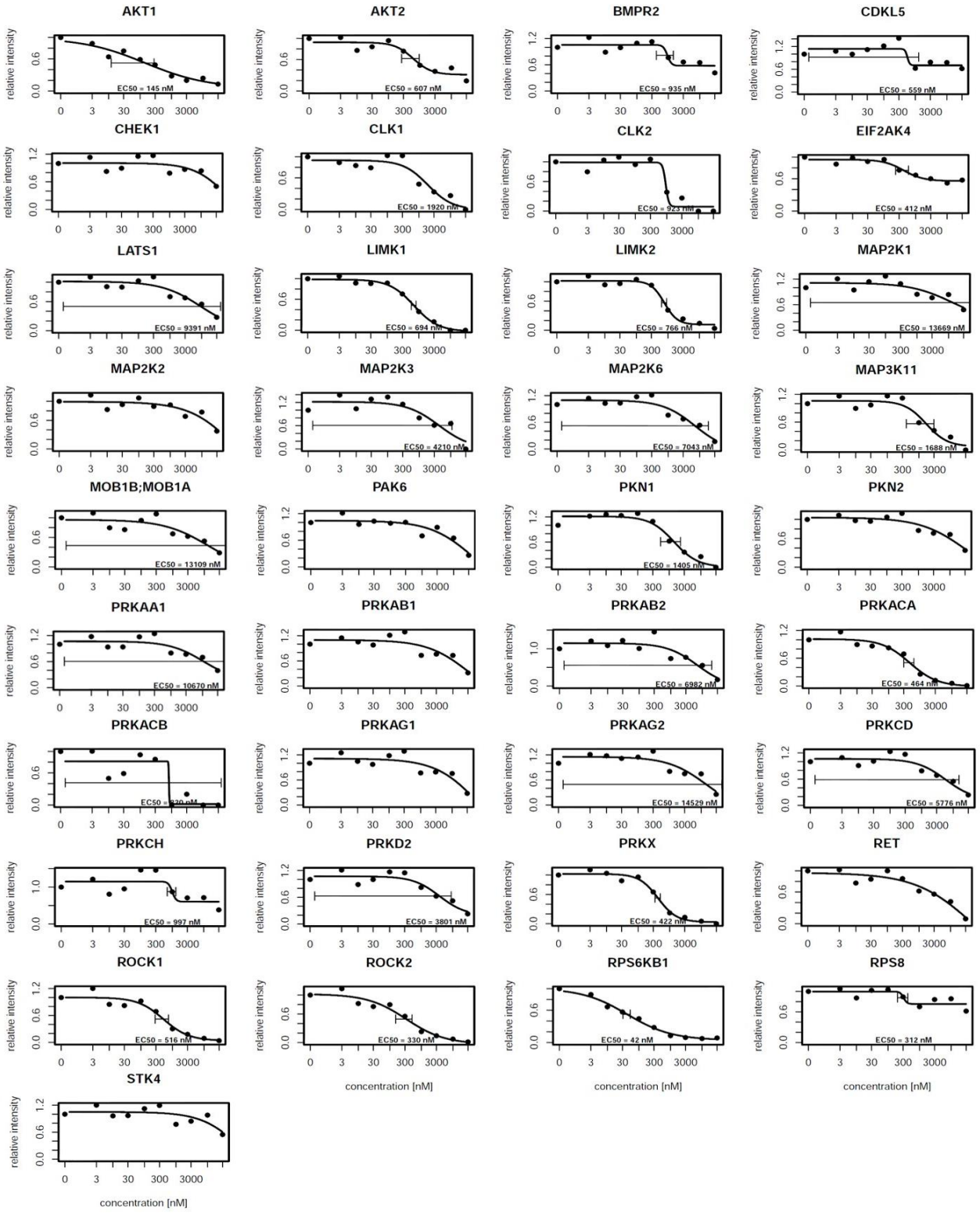

Figure S3: Kinobead target profile of AZD5363.

Dose-dependent binding curves of AZD5363 for all kinase and non-kinase targets identified by kinobeads. The EC50 value is highlighted for each interaction. Data are from a single kinobead experiment.

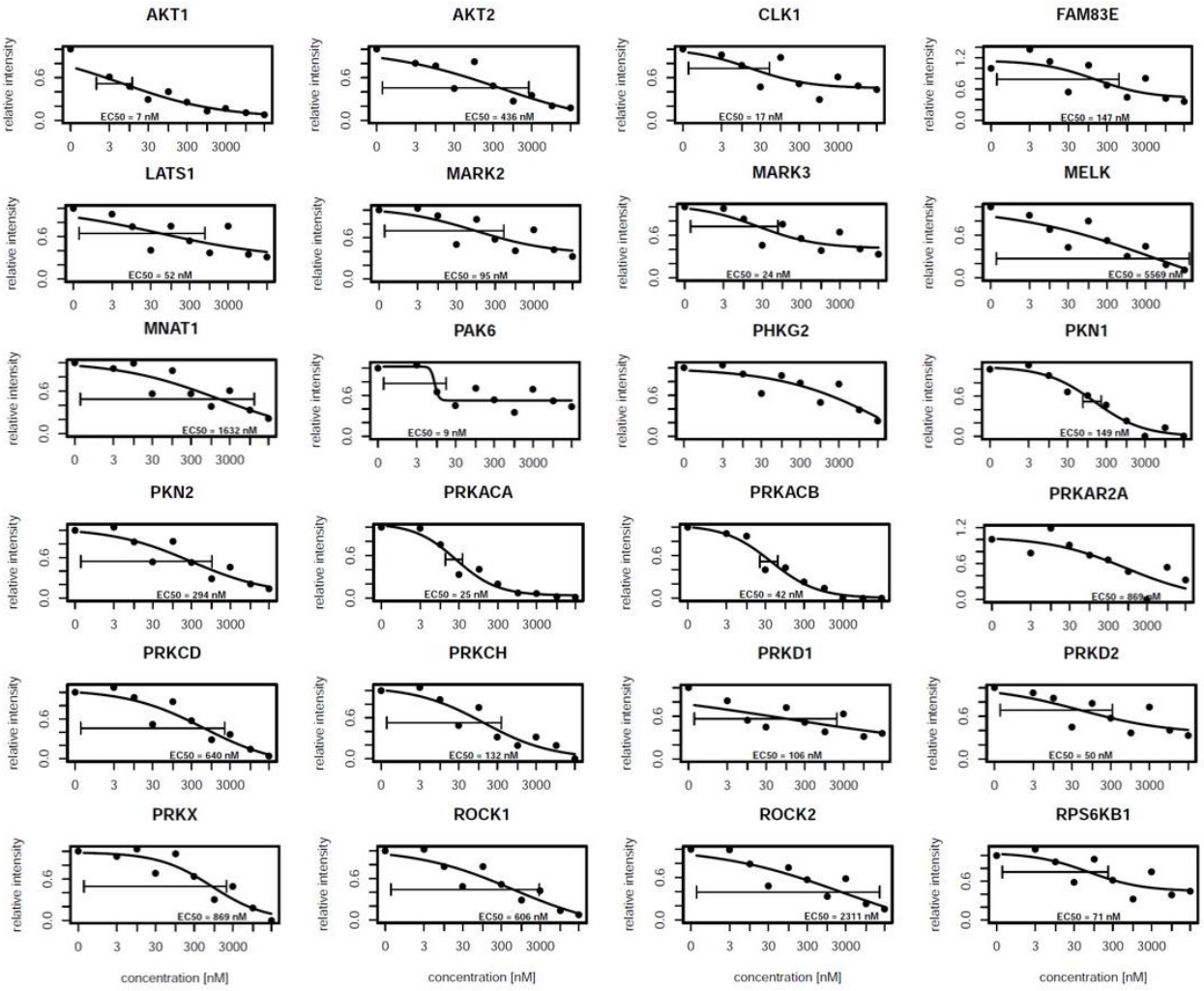

Figure S4: Kinobead target profile of GSK2110183.

Dose-dependent binding curves of GSK2110183 for all kinase and non-kinase targets identified by kinobeads. The EC50 value is highlighted for each interaction. Data are from a single kinobead experiment.

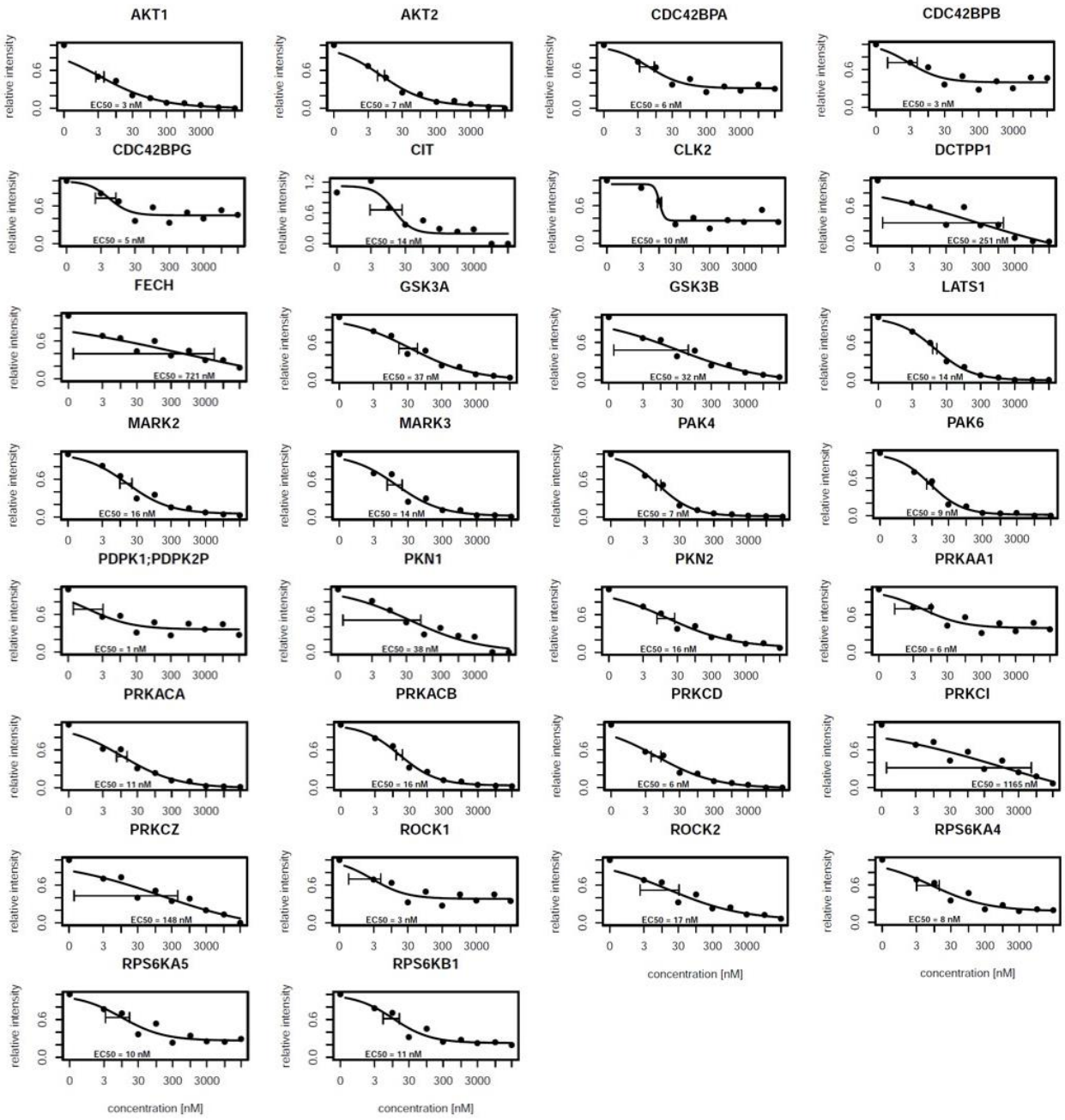

Figure S5: Kinobead target profile of GSK690693.

Dose-dependent binding curves of GSK690693 for all kinase and non-kinase targets identified by kinobeads. The EC50 value is highlighted for each interaction. Data are from a single kinobead experiment.

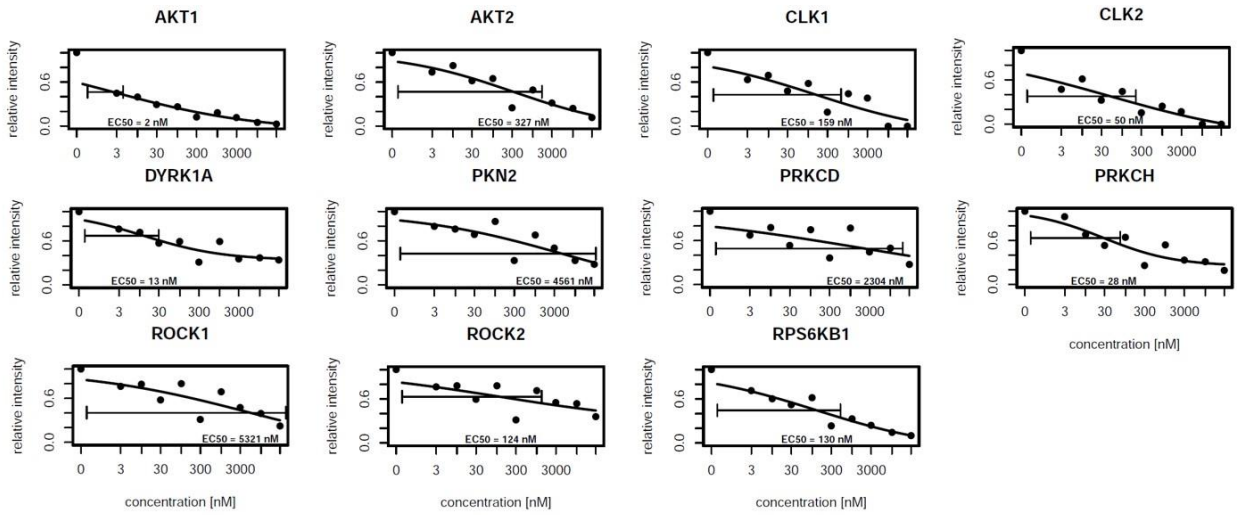

Figure S6: Kinobead target profile of Ipatasertib.

Dose-dependent binding curves of Ipatasertib for all kinase and non-kinase targets identified by kinobeads. The EC50 value is highlighted for each interaction. Data are from a single kinobead experiment.

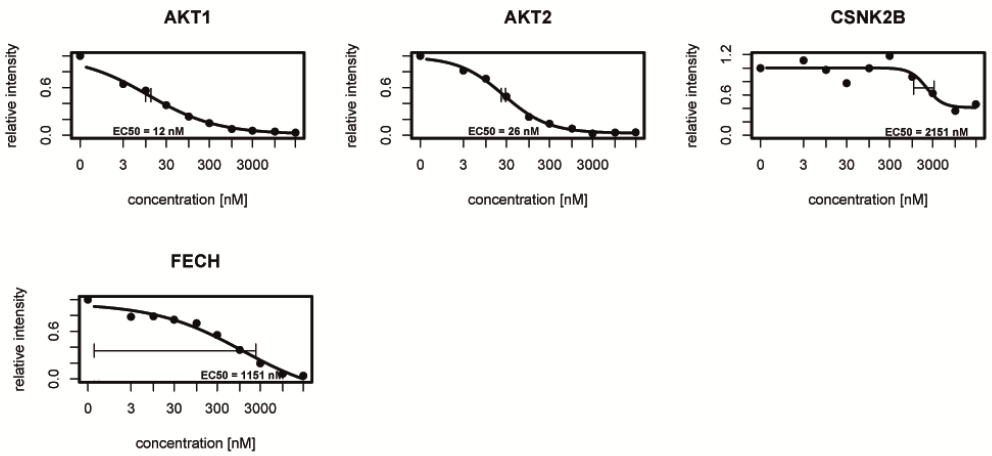

Figure S7: Kinobead target profile of MK-2206.

Dose-dependent binding curves of MK-2206 for all kinase and non-kinase targets identified by kinobeads. The EC50 value is highlighted for each interaction. Data are from a single kinobead experiment.

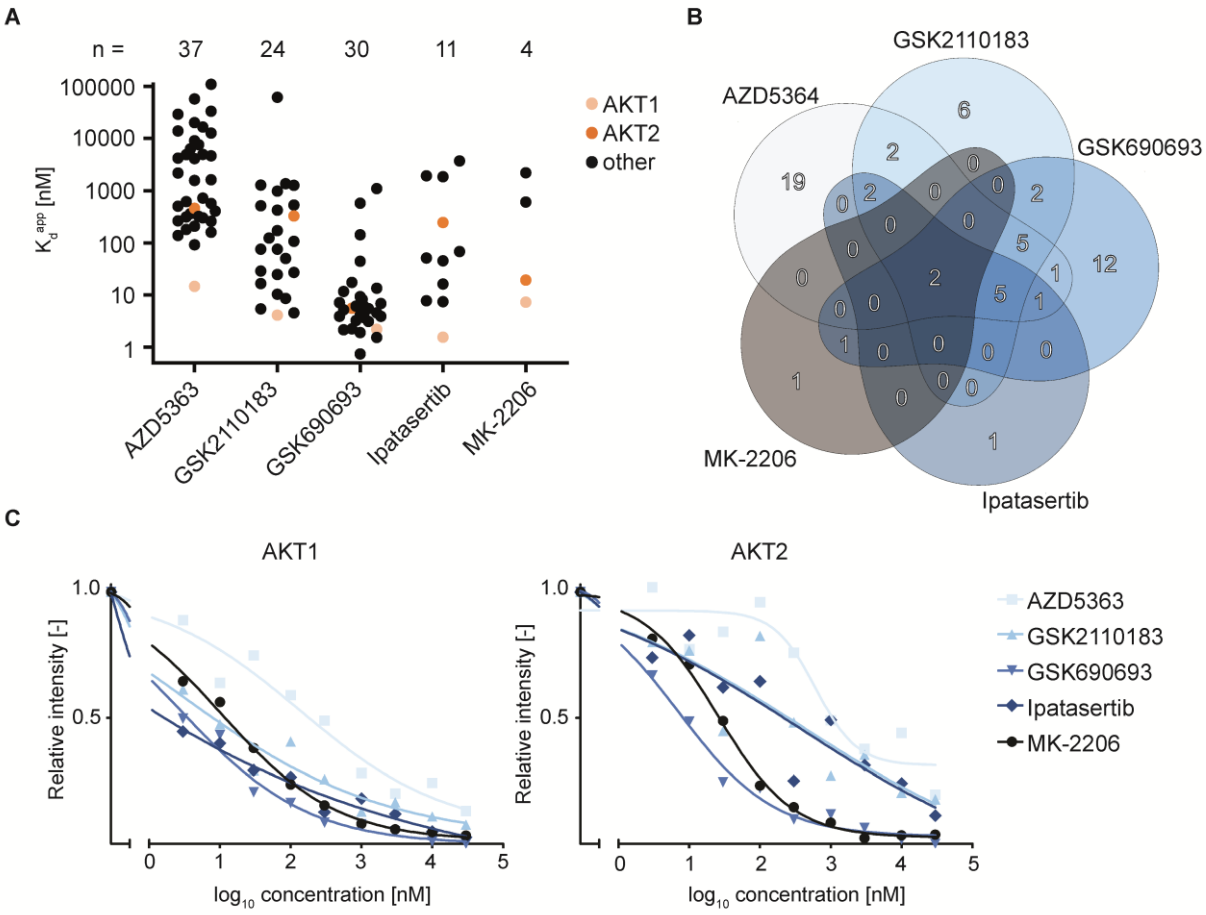

Figure S8: Target deconvolution of the AKT inhibitors AZD5363, GSK2110183, GSK690693, Ipatasertib and MK-2206 using kinobeads.

(A) *Apparent binding constants (K_d^{app}) of target proteins and AKT inhibitors. Each dot represents a protein and AKT1 and AKT2 are highlighted in orange. The number of targets for each drug is indicated at the top.* ***(B)*** *Venn diagram showing the overlap of the targets of the five AKT inhibitors. AKT1 and AKT2 are the only two targets shared by all five inhibitors.* ***(C)*** *Dose-response binding curves of all inhibitors of AKT1 (left panel) and AKT2 (right panel). Data are from a single kinobead experiment.*

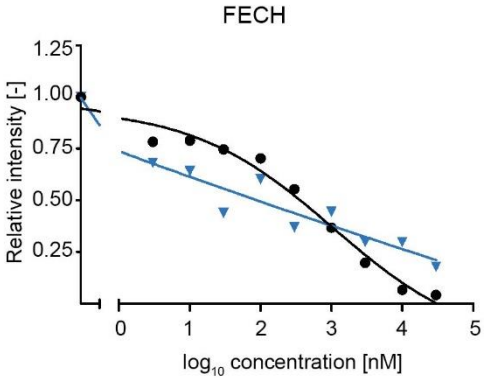

Figure S9: FECH is a target of GSK690693 and MK-2206.

Dose-dependent kinobead-based binding curves of GSK690693 and MK-2206 for FECH. Data are from a single kinobead experiment.

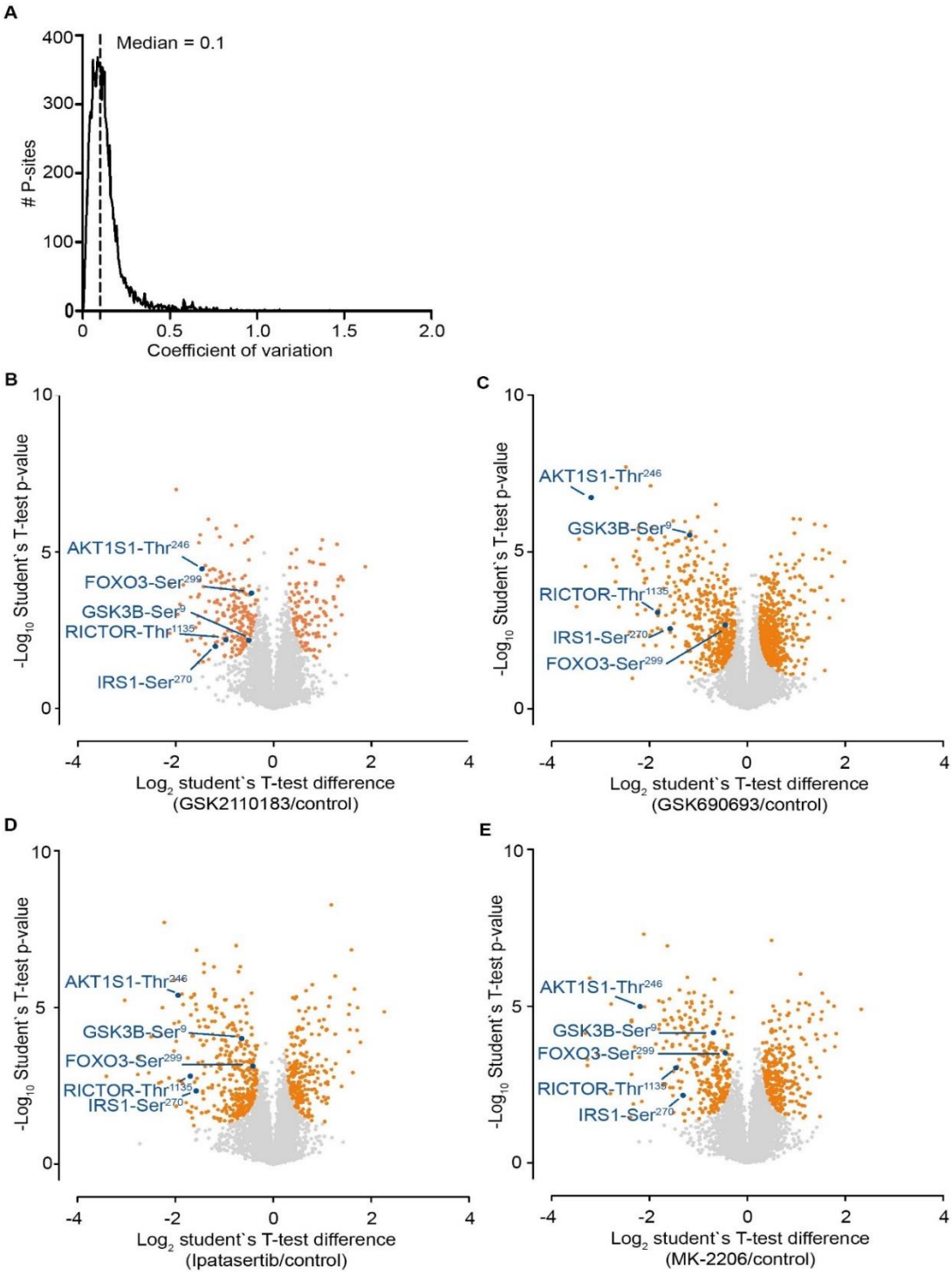

Figure S10: Evaluation of the data quality of the phosphoproteomic dataset.

(A) Histogram of the coefficients of variation of p-site intensities among the control experiments. The median is highlighted by a dashed line. **(B)-(E)** Volcano plots showing the extent and statistical significance of regulation of p-site intensities by GSK2110183 (B), GSK690693 (C), Ipatasertib (D) and MK-2206 (E). Significantly regulated p-sites are marked in orange. Known phosphorylated AKT pathway members (GSK3B-Ser^{9}, FOXO3-Ser^{253}, AKT1S1-Thr^{246}, RICTOR-Thr^{1135} and IRS1-Ser^{270}) are highlighted in blue. Data represent *N* = 3-4 independent biological replicates. Statistical analyses were performed using T-tests (FDR = 0.05, s0 = 0.1).

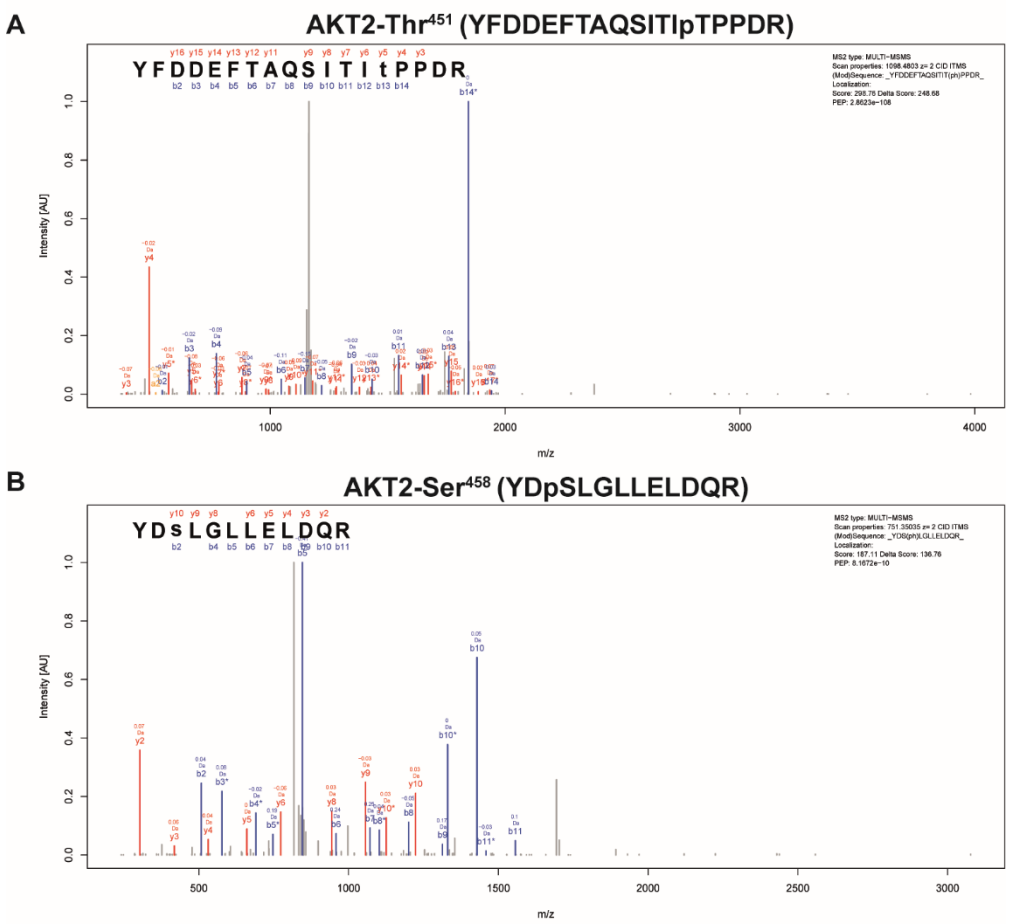

Figure S11: Annotated MS/MS spectra of phosphorylated (A) AKT2-Thr^{451} and (B) AKT2-Ser^{458} peptide.

Scan properties of the MS/MS spectrum and respective scores of the MaxQuant search are shown on the right. The annotated MS/MS spectrum with the highest Andromeda score each was chosen to be displayed.

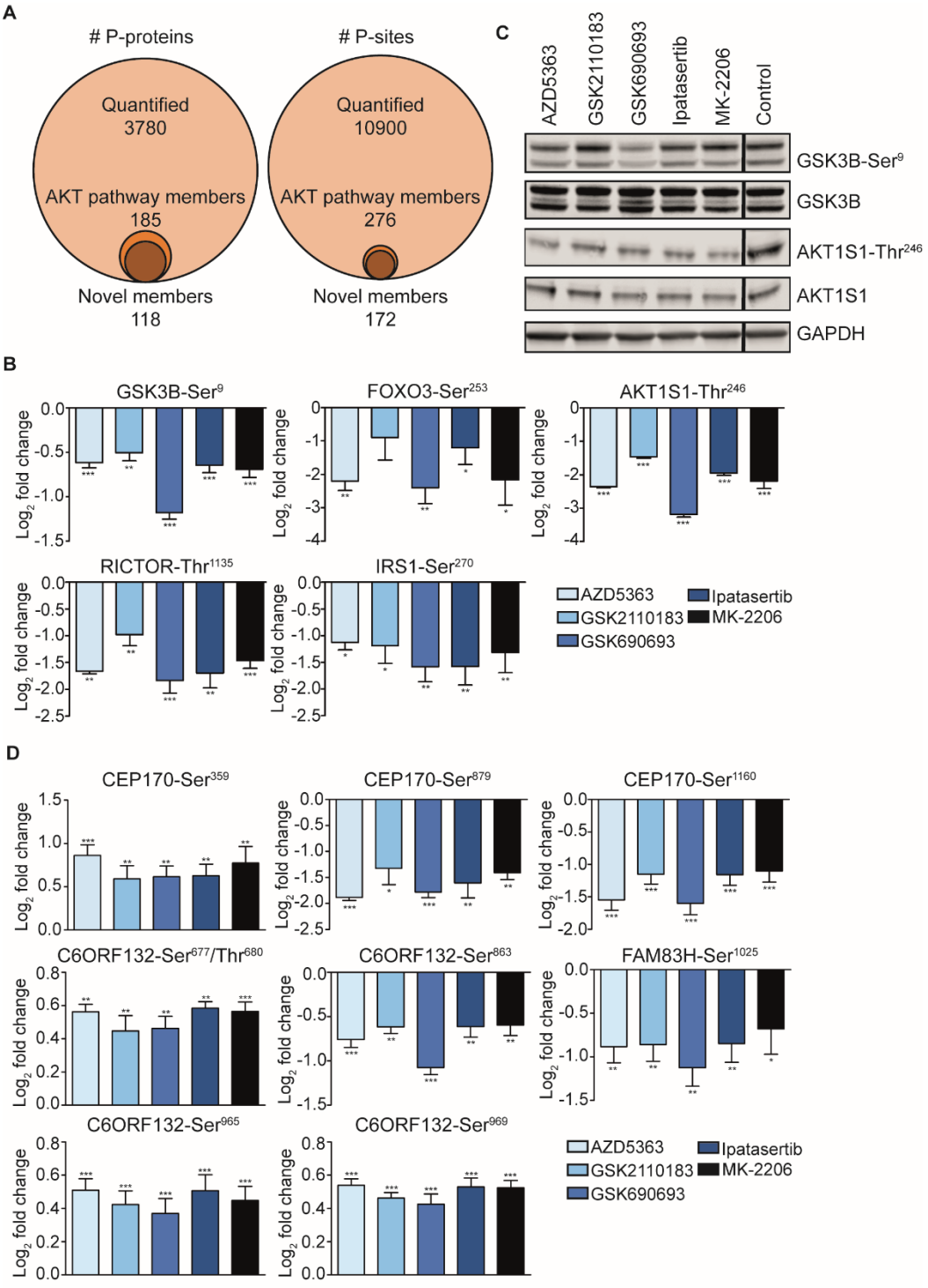

Figure S12: Coverage of known and novel AKT pathway members at the protein and p-peptide level and selected examples of drug-regulated p-sites.

(A) Venn diagrams showing p-proteins (left) and p-sites (right) quantified in all four biological replicates as well as the subsets of the drug-regulated known and novel AKT pathway members. **(B)** LC-MS^3 quantification of phosphorylated known AKT pathway members GSK3B-Ser^9, FOXO3-Ser^{253}, AKT1S1-Thr^{246}, RICTOR-Thr^{1135} and IRS1-Ser^{270} p- in response to AKT inhibitor treatment. **(C)** Immunoblots showing GSK3B-Ser^9, GSK3B, AKT1S1-Thr^{246}, AKT1S1 and GAPDH levels in response to treatment with the five AKT

inhibitors. **(D)** LC-MS^3 quantification of phosphorylated novel AKT pathway members CEP170-Ser^{359}, CEP170-Ser^{879}, CEP170-Ser^{1160}, C6ORF132-Ser^{677}/Thr^{680}, C6ORF132-Ser^{863}, FAM83H-Ser^{1025}, C6ORF132-Ser^{965} and C6ORF132-Ser^{969} in response to AKT inhibitor treatment. Data represent *N* = 3-4 independent biological replicates. Statistical analyses were performed using T-tests (FDR = 0.05, s = 0.1). Error bars represent SD. * $P \leq 0.05$, ** $P \leq 0.01$, *** $P \leq 0.001$.

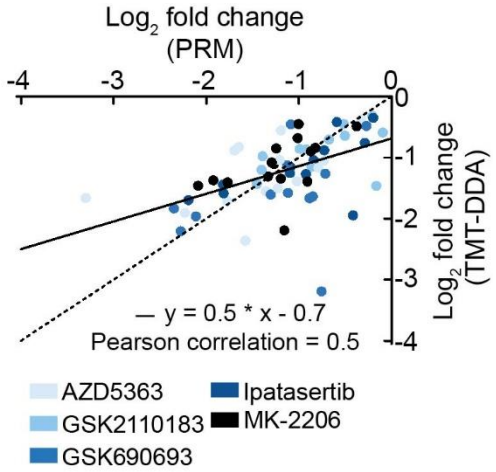

Figure S13: Correlation of p-peptide quantification obtained by TMT-labeling followed by Data Dependent Acquisition of MS data (DDA) vs parallel reaction monitoring (PRM).

Scatter plot of log_2 FC of the 13 p-peptides, which were covered both in the TMT-DDA and PRM datasets. Data points are colored according to which AKT inhibitor was used in the experiment. Linear regression is indicated by a solid line and the Pearson correlation coefficient is shown. The identity line is shown with a dotted line. Data represent N = 3-4 biologically independent experiments. Both types of quantification give broadly similar results, but the TMT data yields consistently lower FCs which can be explained by the so-called 'ratio compression effect' of TMT labeling which is cause by the co-isolation of precursor ions for fragmentation and which cannot be entirely avoided even in LC-MS3 experiments.

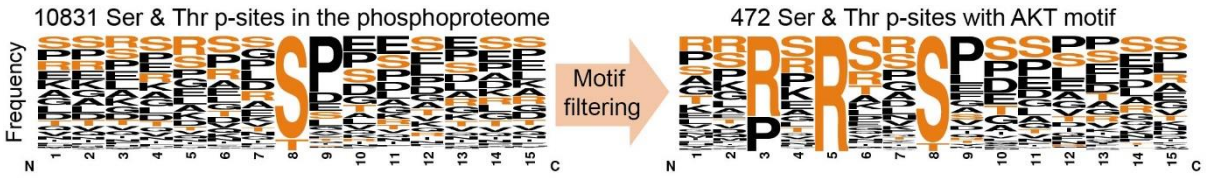

Figure S14: Occurrence of the AKT motif in the phosphoproteomic dataset.

Sequence logo plots showing the amino acid frequency around the 10,831 Ser and Thr p-sites of the complete phosphoproteomic dataset (left) and the subset of 472 p-sites bearing the AKT motif (right). Data represent *N* = 3-4 biologically independent experiments.

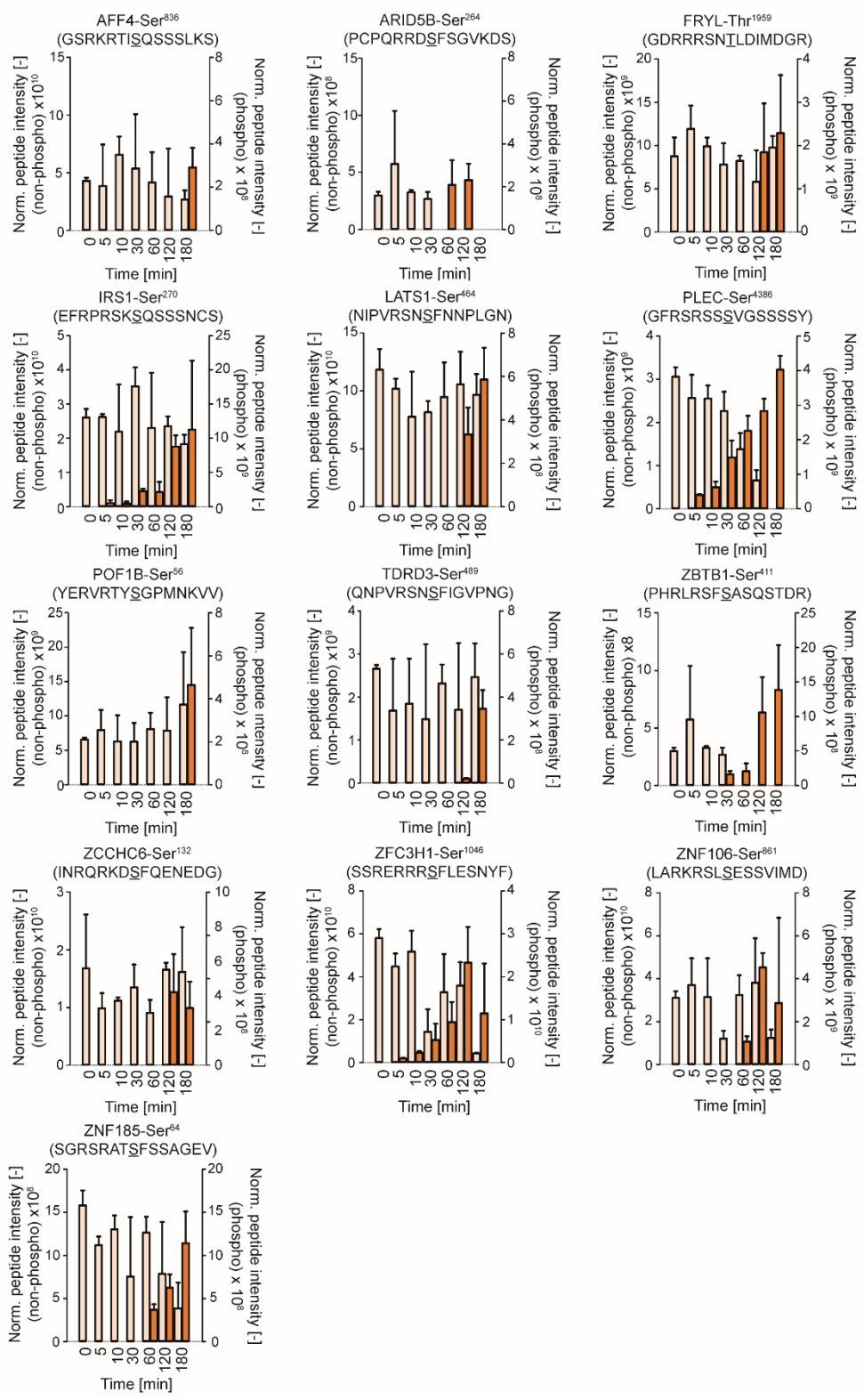

Figure S15: In-vitro kinase assays to confirm novel AKT2 substrates.

Normalized peptide intensities of non-phosphorylated and phosphorylated peptides representing AFF4-Ser^{836}, AIRD5B-Ser^{264}, FRYL-Thr^{1959}, IRS1-Ser^{270}, LATS1-Ser^{464}, PLEC-Ser^{4386}, POF1B-Ser^{56}, TDRD3-Ser^{489}, ZBTB1-Ser^{411}, ZCCHC6-Ser^{132}, ZFC3H1-Ser^{1046}, ZNF106-Ser^{861} and ZNF185-Ser^{64} after 0, 5, 10, 30, 60, 120 or 180 min incubation in

recombinant AKT2 kinase. Data represent $N = 3$ independent experiments. Error bars represent SD.

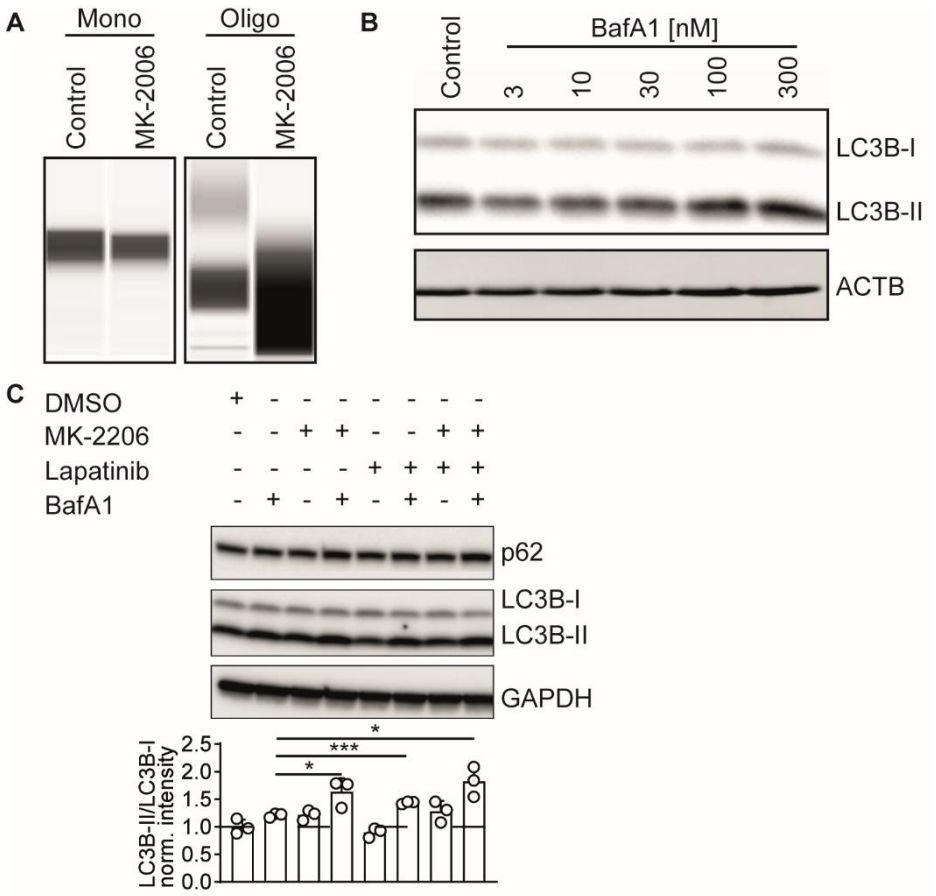

Figure S16: AKT inhibition-induced autophagy.

(A) Immunoblots quantifying levels of ATG4 in its monomeric or oligomeric state in response to MK-2206 treatment. **(B)** Immunoblots showing LC3B-I, -II and ACTB levels in response to titration of BafA1. **(C)** Immunoblots showing p62, LC3B-I, -II and GAPDH levels in response to treatment with MK-2206, lapatinib or a combination thereof. Quantification of the LC3B-II-to-LC3B-I ratio normalized to the DMSO control is shown below**.** Data represent $N = 3$. Statistical analyses were performed using T-tests. Error bars represent SD. * $P \leq 0.05$, ** $P \leq 0.01$, *** $P \leq 0.001$.